

Observations and Bayesian location methodology of transient acoustic signals (likely blue whales) in the Indian Ocean, using a hydrophone triplet

Ronan J. Le Bras,^{1,a)} Heidi Kuzma,² Victor Sucic,³ and Götz Bokelmann¹

¹*Institut für Meteorologie und Geophysik, University of Vienna, Vienna, Austria*

²*Chatelet Resources, Truckee, California 96161, USA*

³*Faculty of Engineering, University of Rijeka, Rijeka, Croatia*

(Received 27 October 2014; revised 19 March 2016; accepted 24 April 2016; published online 12 May 2016)

A notable sequence of calls was encountered, spanning several days in January 2003, in the central part of the Indian Ocean on a hydrophone triplet recording acoustic data at a 250 Hz sampling rate. This paper presents signal processing methods applied to the waveform data to detect, group, extract amplitude and bearing estimates for the recorded signals. An approximate location for the source of the sequence of calls is inferred from extracting the features from the waveform. As the source approaches the hydrophone triplet, the source level (SL) of the calls is estimated at 187 ± 6 dB re: $1 \mu\text{Pa}$ -1 m in the 15–60 Hz frequency range. The calls are attributed to a subgroup of blue whales, *Balaenoptera musculus*, with a characteristic acoustic signature. A Bayesian location method using probabilistic models for bearing and amplitude is demonstrated on the calls sequence. The method is applied to the case of detection at a single triad of hydrophones and results in a probability distribution map for the origin of the calls. It can be extended to detections at multiple triads and because of the Bayesian formulation, additional modeling complexity can be built-in as needed. © 2016 Acoustical Society of America. [<http://dx.doi.org/10.1121/1.4948758>]

[TFD]

Pages: 2656–2667

I. INTRODUCTION

Blue whales, *Balaenoptera musculus* (*B.m.*), are the largest animals that have ever lived on earth. They are a charismatic favorite of the public possibly due, in part, to the fact that they sing. Although the reason for their vocalization is still not completely understood, there are hints that only male blue whales sing (McDonald *et al.*, 2001), suggesting a mating function (Wiggins *et al.*, 2005). Recordings of their intricate songs are often used to inspire awe of the natural world and have even been incorporated into popular music pieces (Lewis, 2013). For an overview of marine bioacoustics, in general, and mysticetes (baleen whales), in particular, see Au and Hastings (2008).

Due to extensive whaling during the first part of the century (Kemf and Phillips, 1995), the population of blue whales, once estimated at several hundreds of thousands, has shrunk to only a few thousand remaining today (Branch, 2007). Happily, that number seems to be steadily rising (Branch *et al.*, 2004), since progressively tighter restrictions on whaling were agreed on by the international community, starting with the entry into force of the Convention on Fishing and Conservation of Living Resources of the High Seas in 1966. Furthermore, McDonald *et al.* (2009) discovered that the average frequency content of blue whale songs has been going down, meaning, perhaps, that individual whales are surviving longer, growing even bigger, and

singing deeper songs. This also implies that the population of the whales and not only the size of individuals may be increasing. A discussion of several different types of blue whales present in the area of the dense Indian Ocean is presented in Samaran *et al.* (2013). They analyzed seasonality of calls for two subspecies, the Antarctic (*B.m. intermedia*) and pygmy blue whales (*B.m. caudica*). The pygmy subspecies they observe had three different types of calls, which they named Madagascar, Sri Lanka, and Australia, and their analysis includes the four acoustic populations. The conservation status of the pygmy subspecies is not known, whereas the Antarctic subspecies seems to number around 2280 individuals (Branch, 2007).

The typical frequency of blue whale songs is in the 15–120 Hz range. While most oceanic hydrophones record at higher frequencies, the hydrophone network of the International Monitoring System (IMS) of the Comprehensive Nuclear-Test-Ban Treaty Organization (CTBTO) is constantly recording in this lower range, listening for undersea nuclear explosions. Whale songs are routinely discarded as noise during data processing at the International Data Centre (IDC). The Baleakanta Project (Le Bras *et al.*, 2013) has proposed to take advantage of more than ten years of historic IMS data by compiling a database of whale songs along with the location and movements of the whales that are singing them. Because open access hydrophone arrays are rare and often sporadic, such a database would be a great asset for researchers studying whales and could prove very helpful in monitoring and aiding their recovery. The advantages of using the IMS network are clear: it is a continuously monitoring system, already gathering data in a systematic way, and could be accessed at minimal

^{a)}Present address: International Data Centre, Comprehensive Nuclear-Test-Ban Treaty Organization, 1400, Vienna, Austria. Electronic mail: ronan.lebras@gmail.com

cost to the scientific community, as has already been demonstrated by several groups (Harris *et al.*, 2009; Samaran *et al.*, 2010; Woolfe *et al.*, 2015).

In order to build the database, it is first necessary to be able to recognize (detect) and isolate (discriminate) whale songs in the data. Because each IMS station is composed of a triad of hydrophones, the arrival times of the songs provide enough information to be able to find an approximate bearing (or *azimuth*) to the whales and, in some cases, an estimate of the speed and direction of their travel. This paper gives the results of a preliminary study undertaken to prove the concept of finding whale songs in IMS data and using it to locate the animals, in this case the animals are in the far-field and a plane wave assumption can be made.

In Secs. II B 1 to II B 3, methods for detection of whale songs in IMS hydrophones are discussed and results are presented from the data processing of a 12 day sequence recorded in 2003 in the Indian Ocean. An enormous amount of information can be obtained using relatively simple processing inspired by traditional processing of seismic signals, encompassing the time-frequency signature of songs to the bearing of singing whales from the recording station.

In Secs. II B 4 to II B 7 of the paper, a method for determining the actual position of a whale (not simply its azimuth) is explored using Bayesian signal processing, which is particularly well suited to the problem at hand. It is not difficult to locate an animal if a song is recorded by at least two widely separated groups of hydrophones and can be positively identified as coming from a single source. The situation becomes more complicated, however, if the only data are from a single array.

Several authors have suggested methods for locating whales with single or multiple hydrophones. A good review of basic methods for this purpose is given in Au and Hastings (2008). They concentrate on higher frequencies such as the ones emitted by smaller cetaceans where the distance range of detections is closer to the instruments. Ocean bottom seismometers (OBS) deployed for geophysical purposes offer an opportunistic way to record large cetacean calls over long periods of time. Soule and Wilcox (2013) tracked fin whales in the Juan de Fuca ridge area of the North East Pacific. The signals, typically pulses with a frequency of about 20 Hz, were recorded on an array of eight seismometers in 2003 and 2004. Clark *et al.* (2013) and Jaramillo-Legorreta *et al.* (2013) assume that the whale is either in the near-field of the station, or a group of whales surrounds a station. Samaran *et al.* (2010) use a hyperbolic method of localization, which is appropriate in their study of whales within a few kilometers of the hydrophones, where a plane wave assumption breaks down.

The method presented here is appropriate for the configurations of IMS hydrophones with the assumption, for the computation of the bearing, that the signal is received from the far field, meaning that the distance between the hydrophones is small compared with the distance from the source of the acoustic call. It will be shown to be effective in locating the animals and estimating the uncertainty in their position. Once their location has been found, it may be possible, at least in some circumstances, to estimate the inherent amplitude of their song.

Figuring out how often whales sing, from where and how loud, is an extremely interesting scientific proposition. The more work that is done in this area, the better our understanding will be of not just the animals, but of how signals propagate in the oceans; the better that understanding, the more precise our estimations of whale locations will be. Consequently, the Baleakanta Project is expected to open up a treasure house of discovery, helpful not only to scientists studying cetaceans, but to those monitoring for nuclear blasts as well, through a better knowledge of acoustic propagation in the neighborhood of the hydrophone arrays. It is with that prospect of multiplying returns in scientific gain that this proof of concept is presented.

II. METHOD

A. Test data

A dense sequence of whale songs was recorded between January 1 and 12, 2003, at the Diego Garcia triad of IMS hydrophones (H08N) in the Indian Ocean. The station, about 190 km northwest of the Diego Garcia atoll, consists of a triangle of hydrophones, named H08N1, H08N2, and H08N3, with an approximate spacing of 2.5 km between hydrophones and placed at the axis of the sound fixing and ranging (SOFAR) channel, about 1000 m deep. Figure 1 shows the location of the group of three hydrophones within the Indian Ocean. For a complete description of the station, which includes this triad plus the other triad H08S, located on the southeast side of the atoll, see Hanson (2001).

The songs in the sequence have a time-frequency signature that is similar to a set of songs reviewed by McDonald *et al.* (2006), who coined the type nomenclature for blue whales based on their songs. No direct or reported visual evidence of the presence of blue whales in the area of the hydrophones at the time of these acoustic observations is available and, therefore, no absolute certainty that these signals are originating from them; however, the signals are so similar to the type 9 signals, that it is assumed that blue whales with these call characteristics are the source of the calls. The time-frequency graph of one song, recorded on January 7 at the H08N1 member of the H08N triad, is shown in Fig. 2, alongside a modified version of Fig. 5(d) from McDonald *et al.* (2006). The similarities are very apparent. The songs have durations of about 45 s starting with 15 s of down sweep from 40 to 30 Hz followed, 15 s later, by a monotonal 20 Hz call. Sousa and Harris (2015) describe two distinct types of signals observed during a time period completely including ours and at the same set of hydrophones. They call the two distinct types Diego Garcia Downsweep (DGD) and Diego Garcia Croak (DGC), and cautiously attribute both types to blue whales, with a higher degree of certainty for the DGD signal, which is more frequent, especially at the triad where we both observe them. Their description of the DGD type corresponds very closely with our observations. They observed them at both the H08N and H08S triads, the second component of the Diego Garcia hydroacoustic station. Thus, by visual inspection and comparison with both the signals displayed as type 9 calls by McDonald *et al.* (2006) and the DGD signal of Sousa and

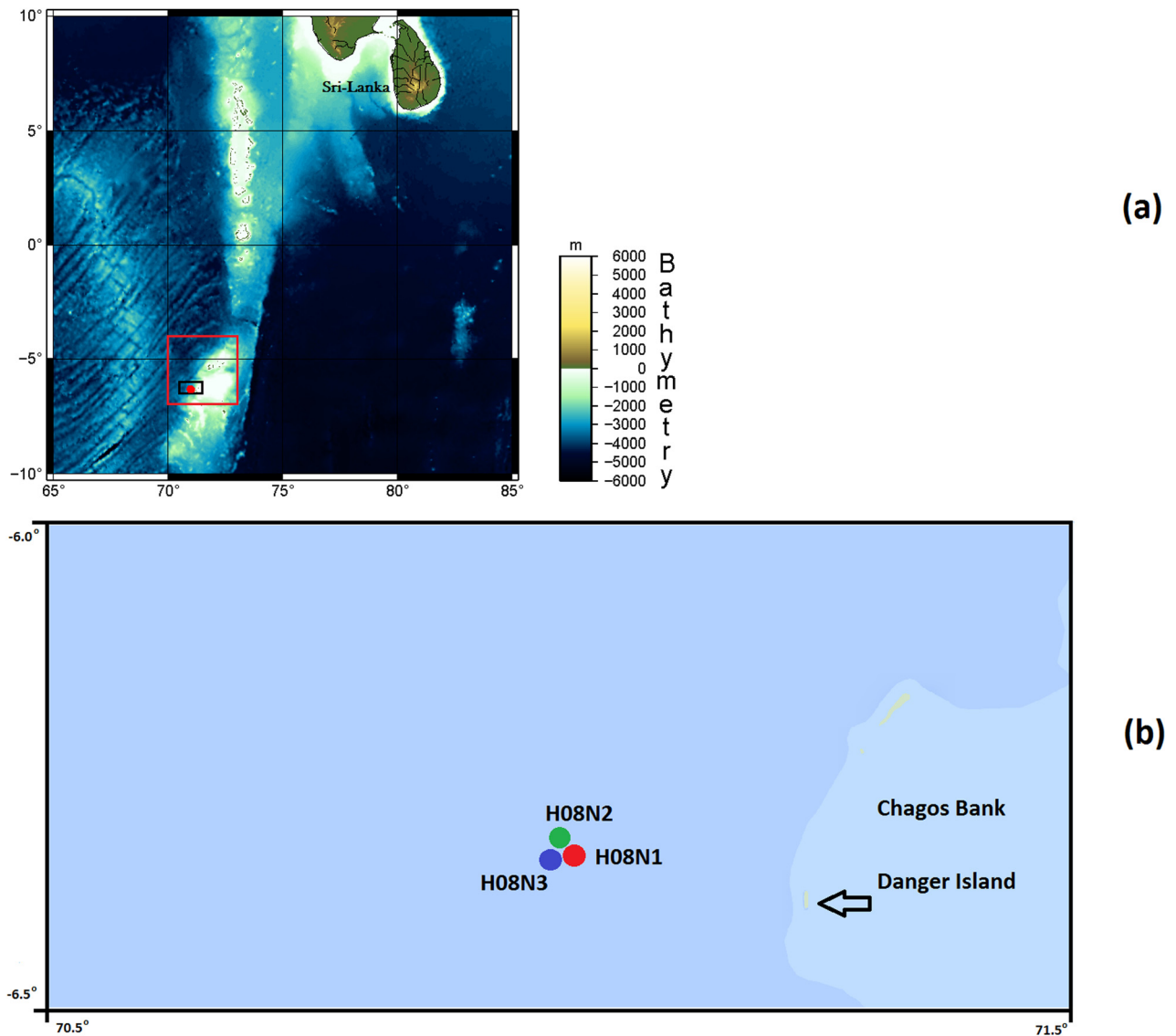


FIG. 1. (a) (Color online) Contextual map in the Indian Ocean for the location of the triad of hydrophones used in this study with, in particular, the southern tip of India and the island of Sri Lanka. The dot within the black rectangle shows the location of the H08N hydrophone triad. Map produced using the GMT software (Wessel and Smith, 1991). (b) Inset map showing the precise location of the three hydrophones: H08N1, H08N2, and H08N3 of the H08N triad station of the IMS. Its location on Fig. 9(a) is shown by the black rectangle.

Harris (2015), the observed signals are assumed to be type 9 calls and follow both publications in attributing them to blue whales, although no one has yet established a link between these types of signals and a visual observation of blue whales. Although they do not report on the presence of whales with this type of call, four different types of whales have been observed in the Indian Ocean on another set of temporarily deployed hydrophones by Samaran *et al.* (2013), none of which, however, were present in January of 2003 according to their paper. This would then mean that there are at least five acoustic types present in the Indian Ocean.

B. Data processing

1. Whale song detection and discrimination

In order to detect whale songs in the IMS hydrophone recordings, the signal was first bandpass filtered using a

fifth-order, 15–60 Hz Butterworth filter appropriate for isolating the frequency bands of type 9 whales. After that, a short term average over long term average (STA/LTA) non-linear filter was applied, which computes the ratio of energy averaged over 1 s of signal to the average energy of 10 s of signal. When no transient signal is present in a time interval, this filter has a value of 1, since the STA and LTA have the same value. When a transient signal is present, the value of the ratio increases. A threshold was applied to the STA/LTA trace to determine the time of detections for the transient signals. This threshold can be interpreted as a signal-to-noise ratio (SNR), and an example with a SNR of 2 is shown on Fig. 3 and a SNR of 2.5 was used to make the detections shown in Fig. 4(a). The filtering sequence was applied to each of the three hydrophones in the station triad. Figure 3 shows an example of filtered trace and STA/LTA traces for the three hydrophones, with the dots indicating the location of the time picks for the signal shown. A hydroacoustic

Hydrophone H08N1, January 1, 2003 at 00:46:35

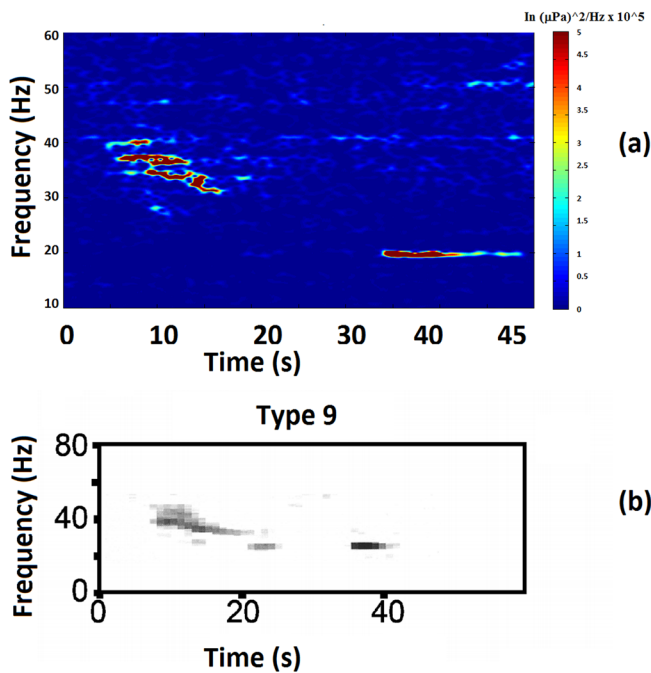


FIG. 2. (a) (Color online) Spectrogram for a whale call recorded on 1 January, 2003, starting at 00:46:35. The amplitude of the spectrogram is in $\mu\text{Pa s}$. This call is typical of South West Indian Ocean type 9 tentatively attributed to blue whales as described by McDonald *et al.* (2006). (b) Reproduced with permission from the first author, and modified from Fig. 5(d) of McDonald *et al.* (2006). The vertical axis is frequency in Hertz and the horizontal axis is in seconds. This is one of two type 9 calls that McDonald *et al.* (2006) show in their figure.

association group (HAG) was registered if all three of the hydrophones registered detections above the same threshold (Hanson *et al.*, 2001). A HAG is more simply called an *arrival* following the IDC seismic standard terminology, meaning that the HAG is the detected arrival of a signal from a signal source. The arrival times at various measurement instruments (such as the three members of the hydrophone triad) will be different depending on the distance and azimuth to the source. This method of detection and arrival determination and terminology is inspired from the detection methods used at the IDC on the waveform data from the IMS global seismic and hydroacoustic network (Laney *et al.*, 1999; Hanson *et al.*, 2001). The method of detection, with three absolute times picked on the trace, also gives us the differential times of the picks at the three hydrophones and, therefore, a means to determine a direction of propagation for a plane wave.

Once an arrival was identified, a Fourier spectrum was computed on the 50 s segment of data immediately following the initial detection. The spectral amplitude average was computed in frequency bands $b_1 = 15\text{--}25$ Hz, $b_2 = 30\text{--}50$ Hz, and $b_3 = 50\text{--}60$ Hz. If the ratio b_2/b_1 was >1.05 , then the signal was positively identified as a potential type 9 whale song. This ratio was determined by observing ten spectra and by trial and error on a 1 h sequence containing whale calls, as well as earthquake signals also detected by the STA/LTA detector, until the value of 1.05 was determined to maximize true detections and minimize false detections (such as the

earthquake signals). Clearly, this step would benefit from further refinement, added parameters and, perhaps, more sophisticated classification methods (Russell and Norvik, 2010).

2. Directional analysis

Two methods were developed for this study and explored as a means of computing the differential times of arrival of the wave front at the three hydrophones. This, in turn, will allow us to identify the direction of propagation of the wave front of the signal emitted by the whale and establish a bearing for the whale using the assumption of horizontal plane wave for a far-field source. The first method is to use the differences in absolute times of the detection of an arrival. The second method is to use relative arrival times determined by the cross correlation of signals received at the individual hydrophones. The time differences between hydrophones are different for the two techniques, but once the time differences are computed, the same method is used to obtain a direction. Figure 3 illustrates the computation on an example and the resultant two different directions.

The problem with both methods is that the propagation characteristics of acoustic signals in the ocean are complex and can change significantly even on the scale of the separation of hydrophones (2.5 km), distorting both detection times and the signal itself. Figure 5 shows an example of distorted Green's functions as received by two theoretical hydrophones at the depth of the SOFAR channel where whale songs propagate best. They are calculated using the Gaussian beam method (Santos *et al.*, 2010; Rodriguez, 2011) for the distances of 498 km, 500 km, and 502 km. The velocity profile used in this illustration was the theoretical Munk profile (Munk, 1974). Significant amplitude and shape differences between the signals are visible, making the signals difficult to correlate. The reason for this is that the signal originating in one point propagates as separate rays following different paths, some of which encounter velocities faster than others, and arrivals from these different rays interfere with each other. This makes both high-definition time detection and cross correlation difficult.

To overcome this problem in the cross correlation method, an iterative method based on a weighting scheme was used which provides a more robust estimation of relative arrival times than straight maximum amplitude picking. The weighting function is an envelope of the cross correlation within a 10 s window, as shown in Fig. 6. The iterative process is as follows:

- (1) Find the peak of the maximum of the cross correlation envelope and use it as the first approximation of the time delay. Figure 6 shows an example of this starting point (square symbol) for the set of three cross correlation functions for a single detection.
- (2) A weighted average of the time using the envelope values as the weights is computed within a 10 s window centered on the current delay approximation. This will give us a new value of the time delay.
- (3) The process is repeated until there is convergence. Convergence occurs when the time delay moves in time less than half a sampling rate. The converged value of

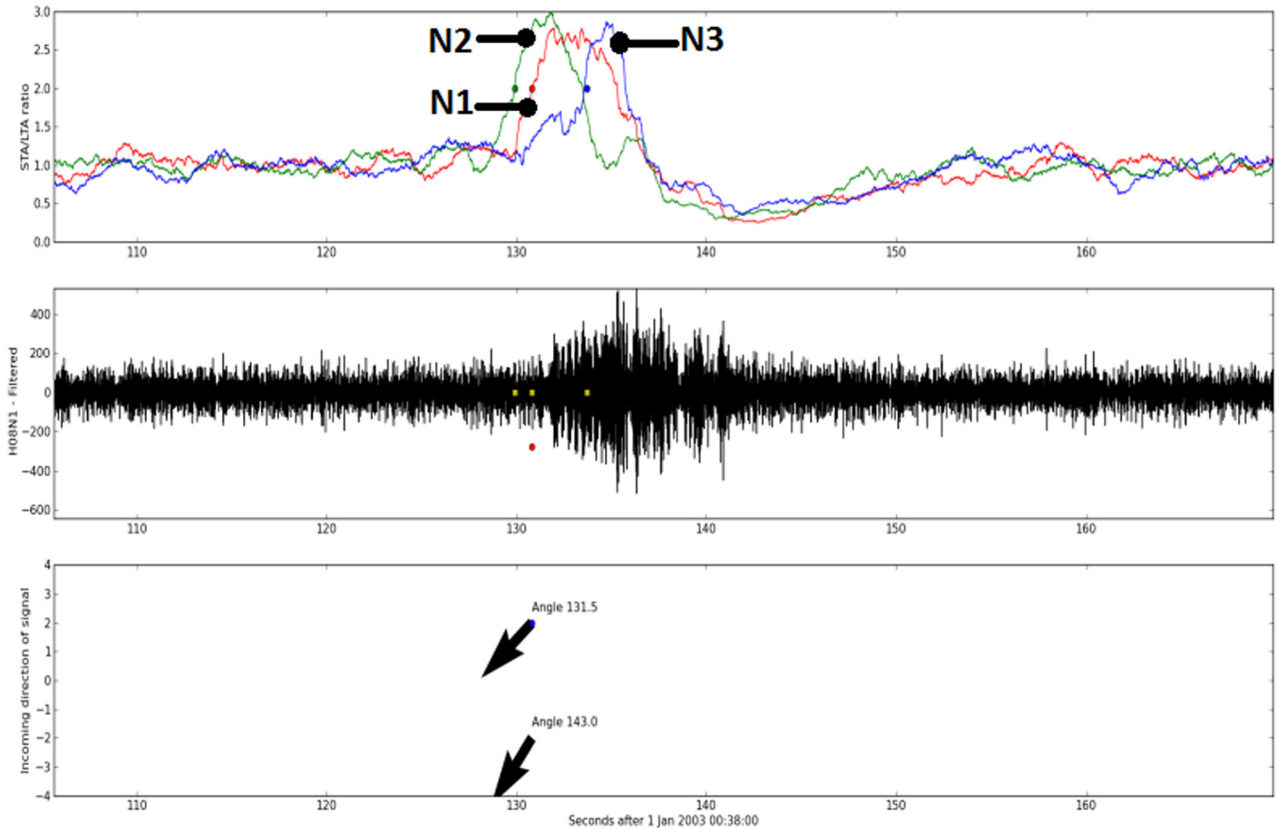


FIG. 3. (Color online) The top trace shows the traces of the STA/LTA filters at each of the three hydrophones of station H08N. They are labeled N1, N2, and N3, which is short for H08N1, H08N2, and H08N3. The dots on the traces are the three time picks made at a STA/LTA threshold of 2 on the STA/LTA traces plus the nominal time at H08N1. Note that the ordinates of the dots are placed at 2 on the STA/LTA plot. The time values for these are reported on the filtered H08N1 trace shown on the middle panel. The bottom panel shows the results of the directional analysis using the two different methods explained in this paper and placed in time at the pick for H08N1. Observe the consistency between the two ways of determining the direction.

the time delay is shown by the circle symbol in Fig. 6. The 10 s window at convergence is also shown by the large box centered on the time delay.

The fact that whale songs are often repeated (up to 60 separately identified calls per hour in a different data set have been observed) helps build robustness into the statistics of the cross correlation. While in the absence of ground truth it is difficult to determine which one of the two direction estimation methods is more accurate, the fact they concord gives us confidence in our direction estimates. The cross correlation technique is favored over the absolute time pick technique because the latter is very approximate and subject to error in the presence of noise. The cross correlation technique is more robust in a noisy context.

3. Results including observations of whale movement

The 12-d dataset from the H08N triplet was processed using the methods described above. It was discovered (Fig. 7) that whale calls were present in these data in bursts that typically lasted a day or two over this period with a maximum frequency of calls of about 20 per hour occurring on January 7. The densest periods are interspersed with periods of silence, or at least quasi-silence, meaning that there were no loud songs. During these 12 d, the location of the signal appears to evolve from a clear initial source to the north to a position directly to the east, then south of east, and finally back to the north. Figure 8 shows the polar coordinate histograms of the detections in groups of 4 d, between 1 and 12 January. Note that the

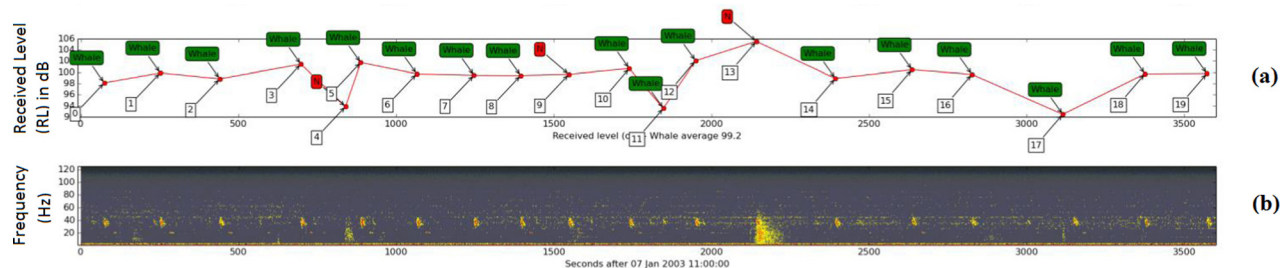
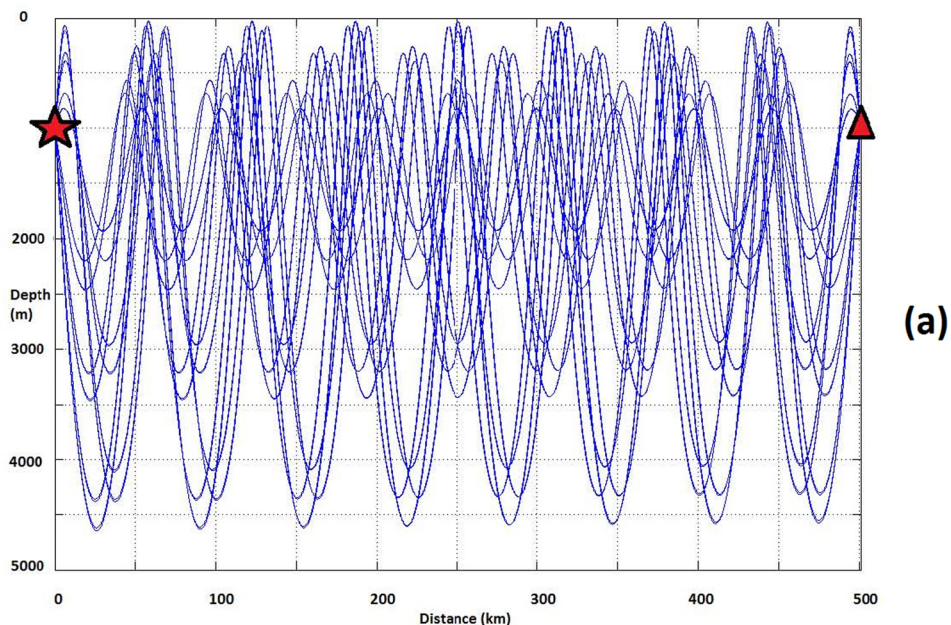
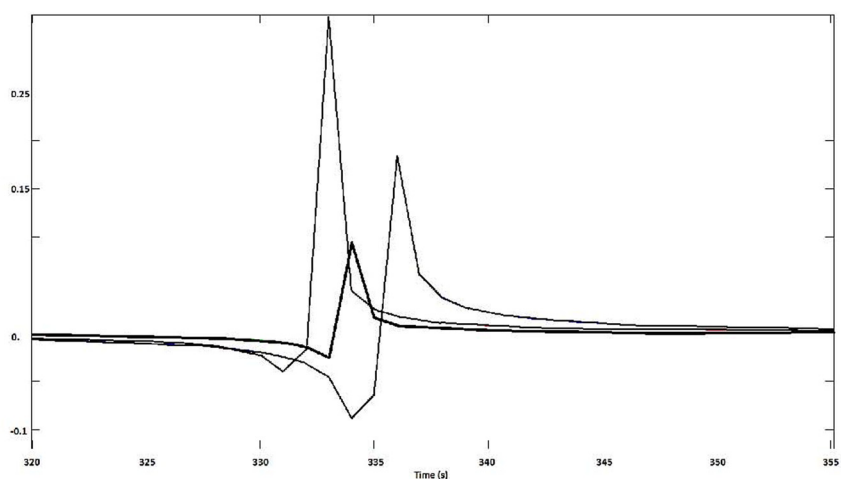


FIG. 4. (Color online) (a) Picks and their log amplitude in a decibel scale with a label resulting from the classification as either “whale” or “N.” The N classification encompasses anything that is not positively identified as a whale. The detection SNR ratio was set at 2.5 in this case. (b) Spectrogram of the raw H08N1 trace between 15 and 50 Hz.



(a)



(b)

FIG. 5. (a) (Color online) Example of eigenrays joining a source and receiver both at the axis of the SOFAR channel. There are only a finite number of paths joining the two points. The location of the source is shown as a star and the location of the receiver as a triangle. The distance between the source and receiver is 502 km. (b) The time series (Green's functions) shown are for receiver distances of 498 km, 500 km, and 502 km. Note that the maximum amplitude has a local minimum at the intermediate distance of 500 km (thickest trace on the figure). The trace for the 502 km distance is the sum of all the Green's functions for the eigenrays shown in (a).

later days show distinctly different azimuths to the signal source, with a large portion of the songs coming from the east-southeast as opposed to the north-northeast from whence they arrived in the first 4 d. The most likely explanation is that these are the bearings of a whale (or group of whales) that were on the move from a northern position to a position to the east of the triad of hydrophones, although it cannot be discounted that different animals or groups of animals at these different locations emit signals in turn.

The time-frequency characteristics of the songs detected during this period are very similar and thus consistent with the hypothesis that all of the songs were coming from the same individual. It is, however, well known that blue whale signals are very similar from one individual to another (Hoffman *et al.*, 2010). Finer frequency and amplitude analysis might indicate that they are originating from a small group instead.

Particularly interesting are the days on which the source of the signal is primarily from the east. This occurs on January 7th, for instance. Directly to the east of Diego

Garcia lies Danger Island where (of course) bathymetry goes to zero. This implies that a whale was singing <25 km from the H08N triad. That the whale was close to the triad is further supported by the observation that (1) the amplitude of the signal was the largest that was observed during the study period; and (2) a number of smaller signals were detected which can be interpreted as reflections or scattering, possibly from the shallow seafloor or from a nearby seamount [Fig. 9(a)]. An accurate bathymetric map is key to unraveling the patterns of diffraction and reflection induced by whale calls and the subject merits further study.

4. Bayesian network model for estimating whale positions

In the above discussion, only the azimuth of whales relative to the recording station was estimated; there was no attempt to determine the whale's actual location. This is a difficult problem, given the complexity of signal propagation in the oceans and the limitation of a recording station with

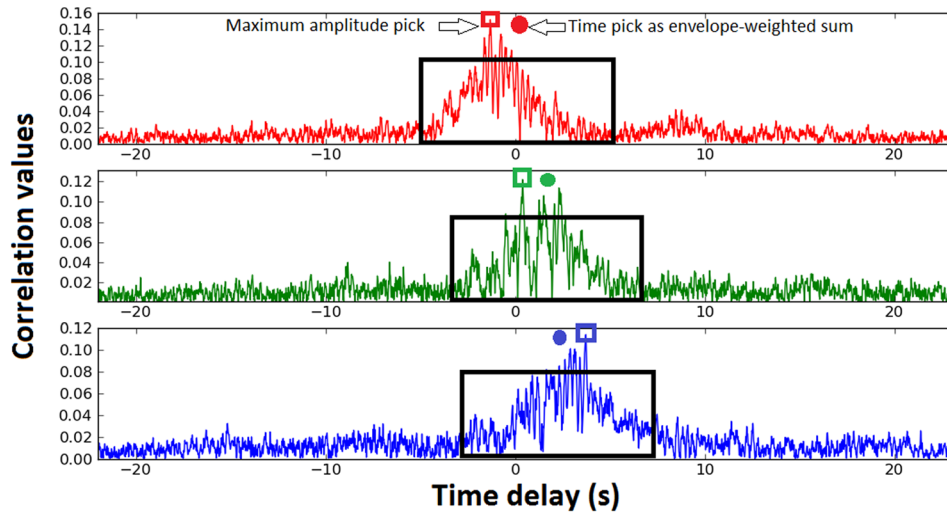


FIG. 6. (Color online) This figure shows the envelopes of the cross correlations for one of the detections. The cross correlations are between the H08N1-H08N2 for the top, H08N2-H08N3 in the middle, and H08N3-H08N1 for the bottom. It is clear that the top trace shows a negative delay while the two bottom panels show positive delays, with the bottom set higher than the middle set. The dots show the location of weighted delay estimates using the envelope of the cross correlation as a weight within a 10 s window. There is one dot per detection. The open square symbols show the location of the peak amplitudes of the envelopes, which are also the starting hypothesis for the delays. The rectangles illustrate the area under which the weighted sum has been computed at convergence. They are centered on the dots.

only three relatively closely spaced hydrophones. It is, however, possible to estimate a location by combining the whale's azimuth with the amplitude of the received signal, although the method relies on being able to accurately model both the amplitude of the signal at its source and transmission losses. To do so without invoking a complex three-dimensional model of oceanic signal transmission, it is necessary to make simplifying assumptions about both the amplitude of the signal and transmission losses.

A Bayesian model is a convenient way to express the relationship between variables in a problem and how they affect each other, particularly when the variables are not well enough known to be expressed as deterministic single numbers. This formulation lends itself nicely to the problem of estimating whale positions because many of the factors affecting signal amplitude are uncertain, including the amplitude of the original signal itself. The Bayesian approach has been used in related problems such as the detection of seismic events using a network of seismic stations (Arora *et al.*, 2013).

Bayes' Law says that the *posterior* probability of whale location, \mathbf{x} (vector of distance and bearing in radial coordinates), and the amplitude of a signal at its source, A_0 , given a measured bearing and amplitude, θ and A , is equal to the product of the *likelihood* of the measurements, or their probability given the whale's location, times the *prior* probability of the location divided by the *prior* probability of the measurements. It is assumed that the signal emitted is isotropic and that the azimuth and amplitude are independent of each other. The equation written out is

$$P(x, A_0 | \theta, A) = P(\theta, A | x, A_0) P(x) P(A_0) / P(\theta, A). \quad (1)$$

By assuming that whales all sing with the same amplitude, that the probability of a whale call being recorded at any bearing and amplitude is uniform, and that the probability of

the location of the whale is also uniform (the whale can be anywhere), then the heart of this equation simplifies to

$$P(x | \theta, A) \propto P(\theta, A | x). \quad (2)$$

Of course, the amplitude of a song probably *does* show variability between individuals, but by making this assumption in order to determine an approximate location of the animal, the amplitude can be dealt with after the fact.

Furthermore, for the particular triad H08N, it is clearly true that a whale cannot be found just anywhere. The knowledge that whales cannot swim on land was already used when interpreting the January 7th sequence of calls above. Nevertheless, the assumption of whale location uniformity is workable in the context of this study as a proof of concept. The Bayesian approach lends itself to very easily add the additional prior probability that the whale has to be in the water (probability of zero on land, uniform in the water).

In radial coordinates, the location of a whale, \mathbf{x} , with respect to a hydrophone is expressed as a distance and true azimuth (as opposed to a measured azimuth) and these are, respectively, r and θ_0 . Making the (rather large) assumption that measured amplitude and bearing is only a function of distance and true azimuth, then

$$P(\theta, A | r, \theta_0) = P(A | r) P(\theta | \theta_0). \quad (3)$$

5. Probability of measured amplitude as a function of distance

The measured amplitude of a signal is its source amplitude minus a transmission loss. For this project, the transmission loss is modeled using a Gaussian ray tracing simulator (Santos *et al.*, 2010), which tracks propagation of simulated

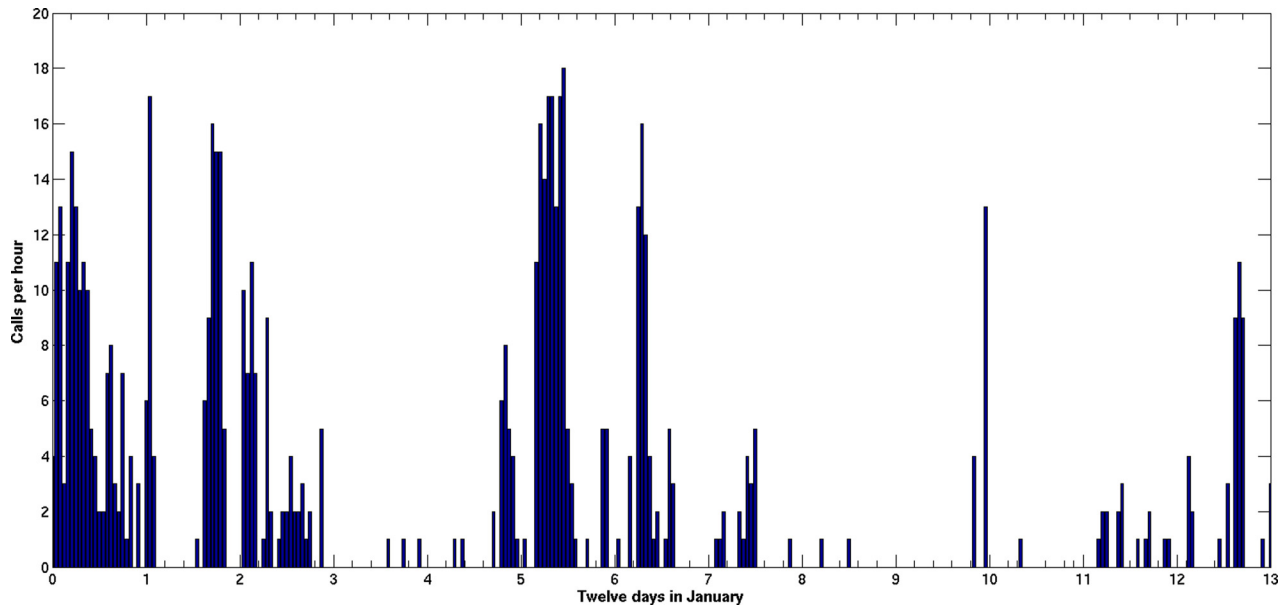


FIG. 7. (Color online) Count of whales per hour during the time period 1–12 January, 2003. The horizontal scale is labeled in days.

signals through the Munk (1974) ocean model. As shown in Fig. 10, the amplitude of a signal decays by ~ 0.16 dB/km within a distance of < 200 km. If the separation between source and receiver is greater than that, the relationship starts to break down, since the amplitude decay is not as rapid after this approximate distance. However, 200 km is an acceptable range for this study. We will show later that all signals from the studied sequence were within this distance from the hydrophones. The complexity of signal propagation in

shadow zones (zones of high attenuation) is ignored for purposes of this paper.

Thus, the predicted amplitude for a signal A_p , expressed as a linear function of distance from its source, r , is

$$A_p = A_0 - 0.16r, \quad (4)$$

where $A_0 = 80$ db, and r is the distance in km.

Deviations from the predicted amplitude are modeled using a log normal distribution, which is suitable for variables

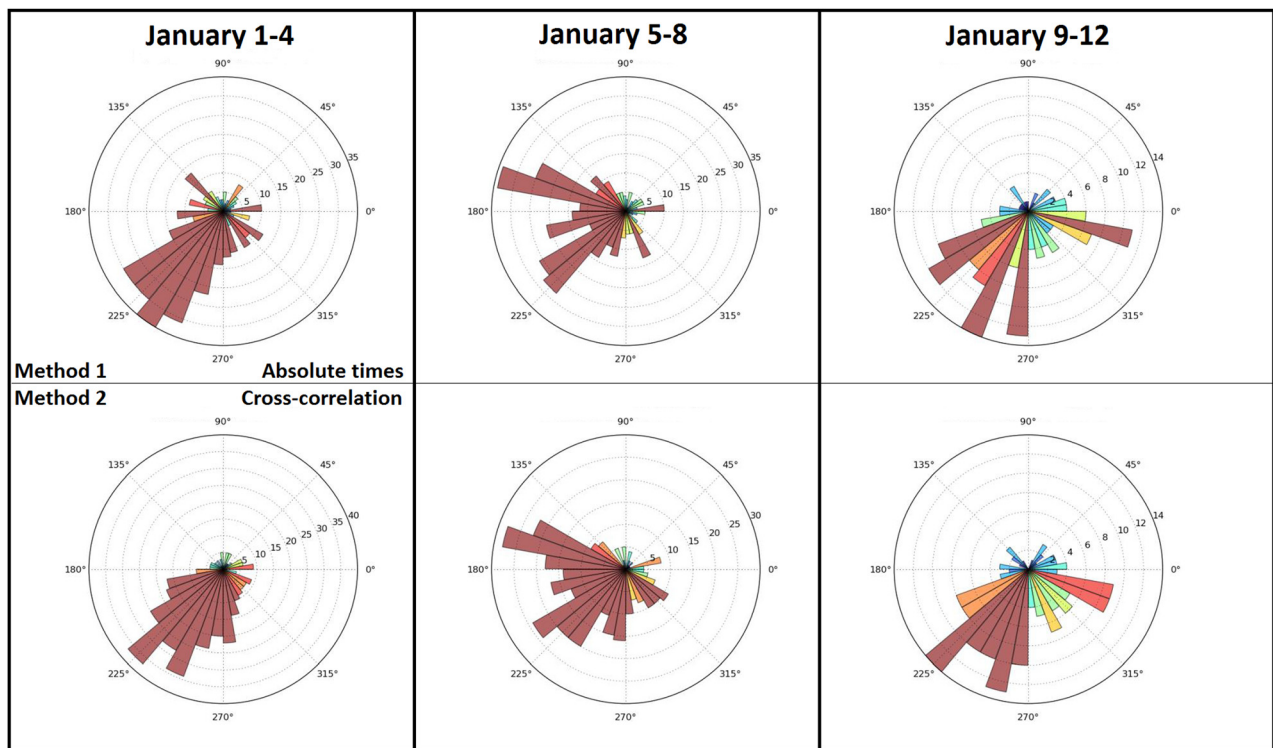


FIG. 8. (Color online) This figure shows bearing determination statistics over 12 d, grouped by bins of 4 d each. The top three histograms show the directional statistics using the absolute time picking method and the bottom histograms show the statistics using the relative time picking method on the cross correlation envelope. A SNR threshold of 2 on the STA/LTA trace was used to compute these statistics. The colors vary with the number of detections in each 10 deg bin.

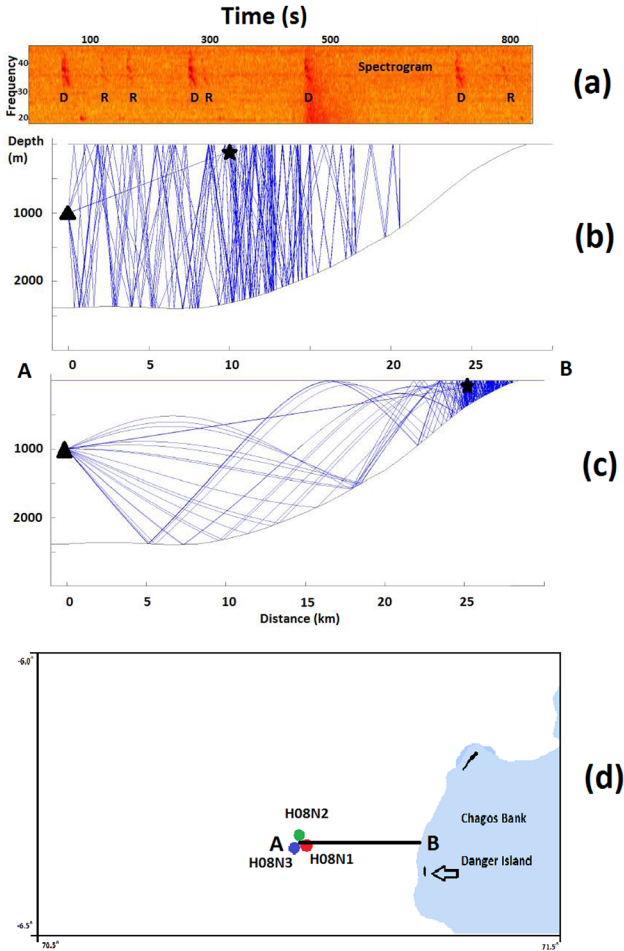


FIG. 9. (a) (Color online) Spectrogram of the raw trace at H08N1 between ~ 20 and 45 Hz for a time of ~ 15 min starting at 11:28 on 7 January, 2003. The presence of signals with lower amplitude than the direct arrival whale calls (at 50 s, 280 s, 470 s, and 710 s) is very clear in this time sequence, at 130 s, 180 s, and again at 300 s and 800 s. These can either be scattered arrivals or more distant animals. (b) Ray paths of scattered waves between a source at 100 m depth and a receiver placed at 1000 m depth for section AB shown in (d). The source is 10 km from the receiver and the velocity profile is the Munk model shown in Fig. 5 (Munk, 1974). The bathymetry of the area due east of the hydrophones is taken from the Google Earth database. [Google Earth version 7.1.2.2041 (10/07/2013). Imagery date 12/14/2015. Data SIO, NOAA, US Navy, NGA, GEBCO.] (c) Same as (b) for a source placed at 25 km and 100 m depth. (d) Map showing the location of the bathymetric section (AB).

that can only have positive values. The formula for this distribution is

$$P_{\mu, \sigma}(A_p) = \mathcal{N}_{\mu, \sigma}(A_p) e^{(-1/2\sigma^2)[\ln(A_p) - \mu]^2}. \quad (5)$$

\ln is the Neperian logarithm function. \mathcal{N} is the lognormal distribution function. The constants σ and μ can be found by fitting the function above to the results of Gaussian ray tracing. Several values were tested visually for the standard deviation and the best fit to the data was chosen. Figure 10 shows an inset with the chosen parameters and the simulated data histogram. The histogram contains all simulated values for A_p . The appropriate values are $\mu = \ln(A_0) = \ln(80) = 4.38$ and $\sigma = 0.08$. A more exact version of these parameters might be found by using a more complicated propagation simulator and ocean velocity model, or by examining data in which

both the source location and amplitude are known. However, for a preliminary study, these numbers are adequate.

6. Property of measured bearing as a function of true bearing

The probability of the measured bearing of a signal is taken to be a von Mises distribution, appropriate for angular variables

$$P_{\gamma, \theta_0}(\theta) = M_{\gamma, \theta_0}(\theta) = \frac{1}{2\pi I_0(\gamma)} e^{\gamma \cos(\theta - \theta_0)}. \quad (6)$$

θ_0 is the bearing to the source without distortion, M is the von Mises distribution function. I_0 is a zeroth-order Bessel function and γ is a standard deviation taken to be 5 deg, based on the standard deviation of bearing estimates of a sequence of calls within 1 h, assuming that the source of the signal is not moving much.

7. Probability of whale location

By integrating, or marginalizing, out the variables A , A_0, θ , and θ_0 in Eq. (1), the following integral formula gives the probability of a source being at any location \mathbf{x} , defined by its polar coordinates r and θ ,

$$\begin{aligned} P(\mathbf{x}|\theta_0, A_p) &= P(\theta, A|\theta_0, A_p) / \left(\int_0^\infty P(A_p) dA_p \int_0^{2\pi} P(\theta_0) d\theta_0 \right). \end{aligned} \quad (7)$$

Substituting the various values from above, this integral gets complicated, but it is readily computed. The denominator is simply the constant 1 when all measured angles and all possible measured amplitudes are equally probable. The numerator becomes the product of two double integrals assuming that A and θ are independent variables

$$\begin{aligned} P(\theta, A|\theta_0, A_p) &= \int_0^{2\pi} d\varphi \int_0^{2\pi} d\omega [M_{\gamma, \theta_0}(\varphi - \theta_0)] [M_{\gamma, \theta_0}(\omega - \theta)] \\ &\times \int_0^\infty d\alpha \int_0^\infty d\beta [\mathcal{N}_{\sigma, \mu}(\alpha - A)] [\mathcal{N}_{\sigma, \mu}(\beta - A_p)]. \end{aligned} \quad (8)$$

This result is a probability map such as the one shown in Fig. 11. The expected value of the probability map (the centroid of whale position) can be computed by integrating over all points in the plane

$$E(x) = \int_0^\infty \int_0^{2\pi} P(x(r, \theta)|A_0, \theta_0) dr d\theta. \quad (9)$$

An ellipse can then be computed which encompasses an area of the probability density function whose sum is one standard deviation (a value of 0.68) of a normal distribution. The ellipticity (ratio of large axis to small axis) is set by computing a best fitting bi-normal distribution centered on the expected value and taking the ratios of the variances.

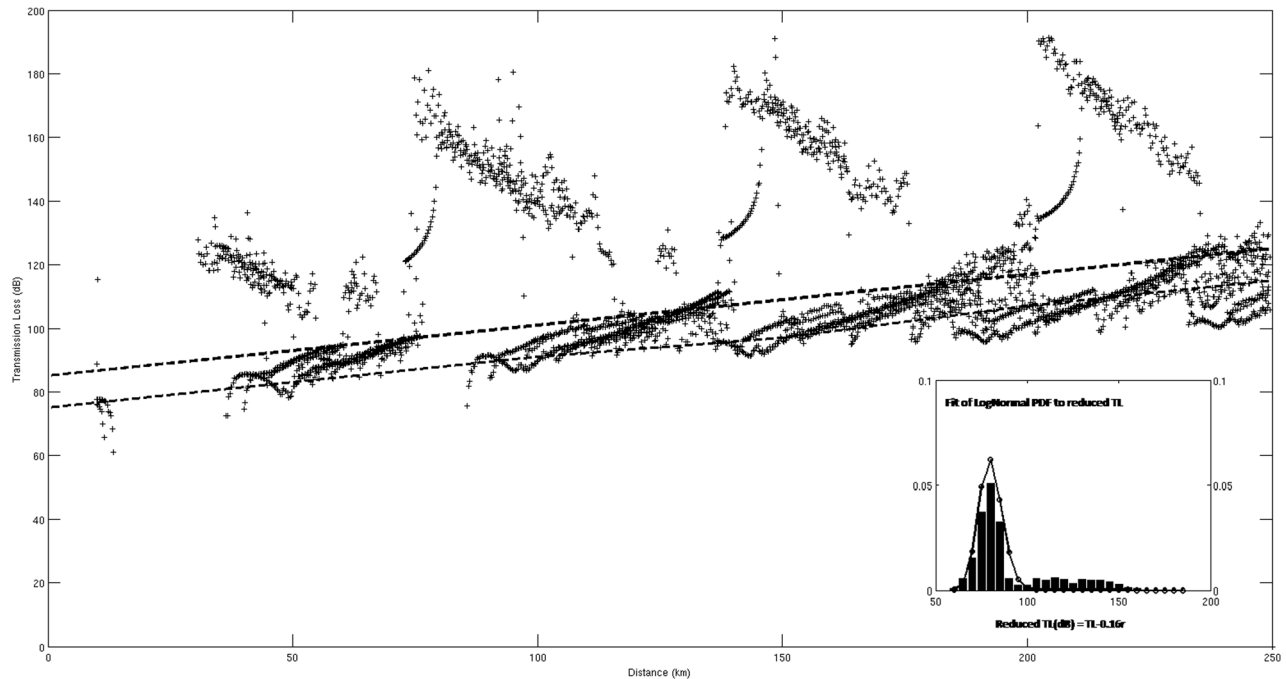


FIG. 10. This shows the transmission loss as a function of distance for a set of four different source depth hypotheses between 0 and 1000 m depth. The inset shows the fit of the lognormal distribution to the variable $A = TL - 0.16r$ for all points on the plot where r is the distance in km. The two dotted lines have a slope of 0.16 db/km.

III. RESULTS

A. Detection and discrimination performance

The performance of the detection and discrimination processing can be evaluated based on a comparison with an independent manual evaluation of ground truth. This was

done on one hour of data starting on January 7, 2003 at 11:00:00 (Fig. 9). This data set contains 18 type 9 calls with high SNRs, one very distinct call with lower SNR (at about 1800 s), and several weaker signals, which may either be reflections or distant sources, and fall below the SNR detection threshold. If the 19 detectable signals are taken as the ground truth, then there were no false positive and two false negatives. This is a short segment compared to the 12 d studied and, furthermore, the noise background is low during this hour, so that the results may be biased toward fewer missed detections. This hour of data does not include signals susceptible to be confused with the type 9 calls, and this may explain the absence of false positives. This may not be the case always and, in particular, other whale call types might also pass this simple discriminant.

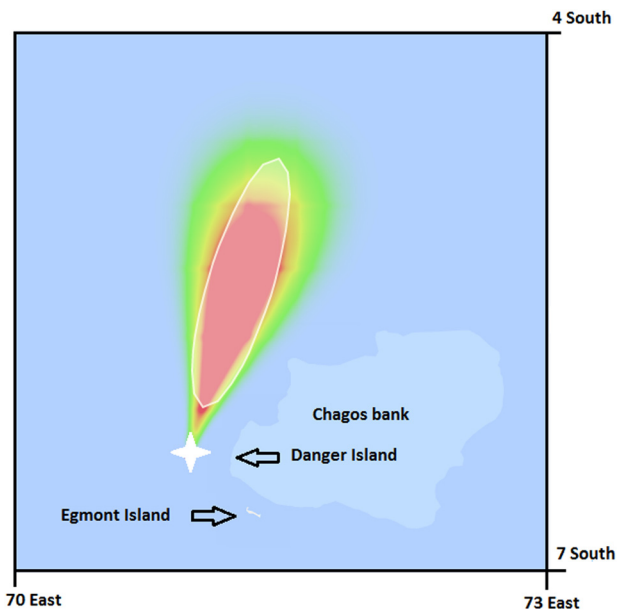


FIG. 11. (Color online) Map of the probability distribution function (PDF) for the location of the whale on January 1, 2003. The map shows the area between 70 and 73 deg east in longitude and between 7 and 4 deg south in latitude, also shown on the contextual map of Fig. 1 as the red square. Also shown is the ellipse centered at the expected location value (not the maximum of the PDF) and corresponding to a probability of 0.68 (1 sigma.) See text for further description.

B. Source level estimation

By rearranging Eq. (4), the amplitude of the source of a signal, A_0 , can be expressed as the amplitude of a received signal A plus whatever transmission loss has occurred. Once the location of a whale has been recovered and the transmission loss can be estimated, then it is possible to estimate the native amplitude of its song.

On January 7th, it was known that the singing whale was between the hydrophones and the island 25 km away. This means that r was somewhere between 0 and 25 km. On that date, the average received amplitude A was 103 dB. The uncertainty in position adds about 1 dB of uncertainty to the 5 dB of uncertainty that was added to the model. Using the rule of thumb in Eq. (4), the amplitude of the source is then estimated to be 187 ± 6 dB re: $1 \mu\text{Pa}-1$ m in the frequency range of 15–60 Hz. For comparison, Samaran *et al.* (2010)

estimated that the songs of the Antarctic blue whale have a source level (SL) of about 179 ± 5 dB re: $1 \mu\text{Pa}\cdot 1\text{m}$ at 17–30 Hz and the pygmy blue whale signal is 174 ± 1 dB re: $1 \mu\text{Pa}\cdot 1\text{m}$ in the band 17–50 Hz (Samaran *et al.*, 2010). Širović *et al.* (2007) estimate the average SL of the Antarctic blue whale at 189 dB re: $1 \mu\text{Pa}\cdot 1\text{m}$, and Gavrilov *et al.* (2011) have an estimate of 179 ± 2 dB re: $1 \mu\text{Pa}\cdot 1\text{m}$ for the most intense pygmy blue whale calls that they observed. The finding is therefore consistent with the song being produced by a loud, big whale and falls within the previously observed ranges for this species.

C. Location of a whale on January 1st

Figure 11 shows the probability map generated from the average amplitude and azimuth of signals arriving on January 1st in the test dataset. The average values for azimuth and amplitude were $\theta = 163$ deg and $A = 93$ dB, respectively. A similar map can be computed for any arrival. By making a movie of the maps, it is possible to monitor the appearances and movements of whales as they are located and recorded by the station (see <http://www.gydatos.org/>, last viewed 8/11/2015).

IV. DISCUSSION

The method we have presented includes assumptions and simplifications. We are assuming that most calls come from a single individual and that the amplitude of the calls at the source is similar for all calls. This is probably justified since the amplitude level of the observations does seem to be quite consistent when we observe a series of 20 or so signals per hour, as is the case for the series shown in Fig. 9 for instance, but may not always be the case. There might also be an azimuthal dependence of the SL while we assume an isotropic source. We have used an amplitude model based on a simulation rather than a simple theoretical decay law such as $1/\sqrt{r}$ for the geometrical decay in cylindrical spreading hypothesis (Samaran *et al.*, 2010).

Since the Bayesian framework lends itself to capturing complicated relationships, much richer models of signal propagation and source characteristics could be built into the algorithm for whale location. Introducing bathymetry into the model where the prior probability is zero where the water depth is < 20 m is quite simple with this method and would take care of modeling the shadow zones blocking acoustic propagation. Introducing reflections is more complex, but may help in refining the position of the animal. For example, if reflections off of Danger Island and other nearby islands were taken into consideration, it might be possible to further refine the position of the whale. Signals in the data from January 7th were consistent with reflections from several islands, although they could also be explained as reflections off of the shallow ocean bottom, or as songs from a different whale located farther away from the hydrophones. This sequence is currently under study.

Furthermore, the simple spectral amplitude ratio method used to classify the particular animal (or animals) in this study as type 9 whales could no doubt be improved by applying modern speaker recognition algorithms such as support

vector machines to improve classification. Research is being undertaken using variants of the Wigner-Ville method (Le Bras and Sucic, 2013) to improve the discrimination of whale calls from other oceanic noise.

V. CONCLUSION

The observations presented in this paper show that, indeed, it is possible to detect whale songs on the IMS network of hydrophones and, with relatively simple processing tools, to estimate the location of the animals. This means that the idea of using the IMS data as the backbone for a catalogue of whale songs and positions is feasible. Further calibrations and refinements to the method will undoubtedly improve precision and understanding of the process as the project proceeds. The models for detection and location of the whales, in turn, will be valuable knowledge for scientists studying cetaceans and will provide groundwork for better observations and understanding of their behavior. It is also expected that as more is known about whale calls, more will be learned about their propagation characteristics, leading to a refinement of oceanic models and even more improvements in data processing.

ACKNOWLEDGMENTS

The hydroacoustic data used in this paper are openly available and were downloaded from the website at <http://www.rds.info> (last viewed 10/8/2015). This work has greatly benefitted from the interactions the first author has had with Emmanuel Ey (Traceo software), John Hildebrand, Danielle Harris, Mark Simmons, Mark Prior, Rüdiger Stempel, and Michael Stachowitsch, and he is extremely grateful for their time and words of encouragement for the Baleakanta endeavor.

- Arora, N. S., Russell, S., and Sudderth, E. (2013). "NET-VISA: Network processing vertically integrated seismic analysis," *Bull. Seismol. Soc. Am.* **103**, 2, 709–729.
- Au, W. W. L., and Hastings, M. C. (2008). *Principles of Marine Bioacoustics. Modern Acoustics and Signal Processing* (Springer, New York), pp. 1–679.
- Branch, T. A. (2007). "Abundance of Antarctic blue whales south of 60°S from three complete circumpolar sets of surveys," *J. Cetacean Res. Manage.* **9**, 253–262.
- Branch, T. A., Matsuoka, K., and Miyashita, T. (2004). "Evidence for increases in Antarctic blue whales based on Bayesian modelling," *Mar. Mammal Sci.* **20**(4), 726–754.
- Clark, C. W., Charif, R. A., Hawthorne, D., Rahaman, A., Givens, G. H., George, J. C., and Muirhead, C. A. (2013). "Acoustic data from the spring 2011 bowhead whale census at Point Barrow, Alaska," in *Scientific Committee Annual Meeting 2013 of the International Whaling Commission*, Jeju Island, Korea, June 3–15, 2013, SC/65A/BRG09.
- Gavrilov, A. N., McCauley, R. D., Salgado-Kent, C., Tripovich, J., and Burton, C. (2011). "Vocal characteristics of pygmy blue whales and their change over time," *J. Acoust. Soc. Am.* **130**(6), 3651–3660.
- Hanson, J. (2001). "Initial analysis of data from the new Diego Garcia hydroacoustic station," in *Proceedings of the 23rd Seis. Res. Sym.*, Jackson Hole, WY, pp. 12–25.
- Hanson, J., Le Bras, R., Dysart, P., Brumbaugh, D., Gault, A., and Guern, J. (2001). "Operational processing and special studies of hydroacoustics at the Prototype International Data Center," *Pure Appl. Geophys.* **158**, 425–456.
- Harris, D., Thomas, L., Hildebrand, J., Wiggins, S., and Harwood, J. (2009). "Estimating whale abundance using sparse hydrophone arrays,"

- Symposium: Estimating Cetacean Density from Passive Acoustics* Scripps Institution of Oceanography, San Diego, CA, July 16.
- Hoffman, M. D., Garfield, N., and Bland, R. W. (2010). "Frequency synchronization of blue whale calls near Pioneer Seamount," *J. Acoust. Soc. Am.* **128**(1), 490–494.
- Jaramillo-Legorreta, A. M., Cardenas-Hinojosa, G., Nieto-Garcia, E., and Rojas-Bracho, L. (2013). "Status of the acoustic monitoring scheme for population trend of vaquita (*Phocoena sinus*) after two sampling periods," in *Scientific Committee Annual Meeting 2013 of the International Whaling Commission*, Jeju Island, Korea, June 3–15, 2013, SC/65A/BRG09.
- Kemf, E., and Phillips, C. (1995). "Whales in the wild," in *1995 WWF Species Status Report* (World Wide Fund for Nature, Gland, Switzerland), pp. 1–24.
- Laney, H., Dysart, P., Freese, H., Brumbaugh, D., Le Bras, R., and Hanson, J. (1999). "Automated detection of underwater explosions by the IMS hydroacoustic network," *J. Acoust. Soc. Am.* **105**(2), 1038–1038.
- Le Bras, R., and Kuzma, H. (2013). "Establishing a Dynamic Database of Blue and Fin Whale Locations from Recordings at the IMS CTBTO hydro-acoustic network," The Baleakanta Project, AGU Fall Meeting Abstracts.
- Le Bras, R., and Sucic, V. (2013). "Individual blue whale recognition. Wigner-Ville time-frequency analysis and preparation for a Kaggle contest," *CTBTO 2013 S&T Conference*, Vienna, Austria, poster.
- Lewis, J. (2013). "Underwater whale sounds—Full 60 minute ambient soundscape," available at <http://www.youtube.com/watch?v=savCAAd6RyPI> (Last viewed 1/23/2016).
- McDonald, M., Calambokidis, J., Teranishi, A. A., and Hildebrand, J. (2001). "The acoustic calls of blue whales off California with gender data," *J. Acous. Soc. Am.* **109**(4), 1728–1735.
- McDonald, M., Hildebrand, J., and Mesnick, S. (2006). "Biogeographic characterization of blue whale song worldwide: Using song to identify populations," *J. Cetacean Res. Manage.* **8**(1), 55–65.
- McDonald, M., Mesnick, S., and Hildebrand, J. "Worldwide decline in tonal frequencies of blue whale songs," *Endangered Species Res.* **9**, 13–21 (2009).
- Munk, W. H. (1974). "Sound channel in an exponentially stratified ocean with applications to SOFAR," *J. Acoust. Soc. Am.* **55**, 220–226.
- Rodriguez, O. C. (2011). "Traceo user manual," available at <http://www.siplab.fct.ualg.pt/models/traceo/manual.pdf> (Last viewed 11/08/2015), pp. 1–69.
- Russell, S., and Norvig P. (2010). *Artificial Intelligence: A Modern Approach*, 3rd ed. (Prentice Hall, Upper Saddle River, NJ).
- Samaran, F., Guinet, C., Adam, O., Motsch, J.-F., and Cansi, Y. (2010). "Source level estimation of two blue whale subspecies in southwestern Indian Ocean," *J. Acoust. Soc. Am.* **127**(6), 3800–3008.
- Samaran, F., Stafford, K. M., Branch, T. A., Gedamke, J., Royer J.-Y., Dziak, R. P., and Guinet, C. (2013). "Seasonal and geographic variation of southern blue whale subspecies in the Indian Ocean," *PLoS One* **8**(8), e71561.
- Santos, P., Rodriguez, O. C., Felisberto, P., and Jesus, S. M. (2010). "Geoacoustic inversion with a vector sensor array," *J. Acoust. Soc. Am.* **128**(5), 2652–2663.
- Širović, A., Hildebrand, J. A., and Wiggins, S. M. (2007). "Blue and fin whale call source levels and propagation range in the Southern Ocean," *J. Acoust. Soc. Am.* **122**(2), 1208–1215.
- Soule, D. C., and Wilcock, S. W. (2013). "Fin whale tracks recorded by a seismic network on the Juan de Fuca Ridge, Northeast Pacific Ocean," *J. Acoust. Soc. Am.* **133**(3), 1751–1761.
- Sousa, A., and Harris, D. (2015). "Description and seasonal detection of two potential whale calls recorded in the Indian Ocean," *J. Acoust. Soc. Am.* **138**(3), 1379–1388.
- Wessel, P., and Smith, W. H. F. (1991). "Free software helps map and display data," *Trans., Am. Geophys. Union* **72**, 441, 445–446.
- Wiggins, S. M., Oleson, E. M., McDonald, M. A., and Hildebrand, J. (2005). "Blue whale (*Balaenoptera musculus*) diel call patterns offshore of Southern California," *Aquat. Mammals* **31**(2), 161–168.
- Woolfe, K. F., Lani, S., Sabra, K. G., and Kuperman, W. A. (2015). "Monitoring deep-ocean temperatures using acoustic ambient noise," *Geophys. Res. Lett.* **42**, 2878–2884, doi:10.1002/2015GL063438.